Version Date: 11:00 PM, 7/1/2009

The Formation and Stability of Carbonic Acid on Outer Solar System Bodies

Z. Peeters[a,b], R. L. Hudson[a,c], M. H. Moore[a], Ariel Lewis[c]

[a]Code 691, NASA Goddard Space Flight Center, Greenbelt, MD 20771
[b]Department of Chemistry, The Catholic University of America, Washington, DC 20064
[c]Department of Chemistry, Eckerd College, St. Petersburg, FL 33711

Manuscript pages: 40 (Text: 16 pages)
Figures: 9
Tables: 6

Abstract

The radiation chemistry, thermal stability, and vapor pressure of solid-phase carbonic acid (H_2CO_3) have been studied with mid-infrared spectroscopy. A new procedure for measuring this molecule's radiation stability has been used to obtain intrinsic IR band strengths and half-lives for radiolytic destruction. Results are compared to literature values. We report, for the first time, measurements of carbonic acid's vapor pressure and its heat of sublimation. We also report the first observation of a chemical reaction involving solid-phase carbonic acid. Possible applications of these findings are discussed, with an emphasis on the outer Solar System.

Key Words: Ices, IR Spectroscopy; Satellites, Surfaces; Cosmic Rays

the closest planet. In each case, carbonic acid may be formed, and for Callisto a tentative detection of H_2CO_3 already has been made (Johnson et al., 2004).

To assess the formation and stability of carbonic acid in the Solar System, it is important to investigate the molecule's physical and chemical properties, but little such work has been published to date. Gerakines et al. (2000) compared the yields of H_2CO_3 made by exposing $H_2O + CO_2$ ice mixtures to ion irradiation (~ 1 MeV H^+) and to UV photons (~ 10 eV). The same researchers measured carbonic acid's intrinsic IR band strengths by the growth of products resulting from UV destruction of H_2CO_3. Earlier work also showed qualitatively that carbonic acid's vapor pressure is lower than that of H_2O, CO_2, and the observed reaction products, since H_2CO_3 is the last of these to sublime under vacuum in the 200 – 250 K region (Moore and Khanna, 1991). A white color is likely for H_2CO_3 made by acid-base chemistry (photographs in Loerting et al., 2000), and the work by Winkel et al. (2007) showed that the x-ray powder pattern of frozen H_2CO_3 is featureless. To our knowledge, little else, if anything, is known of solid-phase carbonic acid from experiments.

In this paper, we reinvestigate the intrinsic IR band strengths of H_2CO_3 and, for the first time, measure this molecule's radiolytic destruction at several temperatures. These new radiation experiments take into account amorphization of the sample. Furthermore, the highest temperature at which destruction measurements are made has been raised from ~10 K to 200 K. Temperature-dependent changes in the position and width of the H_2CO_3 feature at 2618 cm^{-1} (3.82 μm) have been recorded. The first measurements of the vapor pressure and heat of vaporization of pure H_2CO_3 are given, along with the first example of a low-temperature acid-base reaction of the molecule.

Changes in the IR spectra of irradiated ices were followed by Fourier-transform infrared (FTIR) spectroscopy using a Nicolet Nexus 760 instrument. In this setup, the incident IR beam passed through the sample, was reflected by the underlying aluminum mirror, and then passed through the ice a second time, and to the IR detector, for what are sometimes called transmission-reflection-transmission spectra. Measurements were made at 2-cm^{-1} resolution from 5000 to 650 cm^{-1}, averaged over 150 scans.

For studying the vapor pressure of H_2CO_3, the compound first was made by an acid-base reaction between a 1 molar solution of HBr (Sigma-Aldrich) and a 0.1 molar solution of $KHCO_3$ (Sigma-Aldrich), similar to the technique of Hage et al. (1993). A few microliters of the $KHCO_3$ solution were injected through a septum, using a syringe, onto a KBr substrate at 10 K, attached to the tail section of a closed-cycle helium cryostat. Next, a few microliters of the HBr solution were injected the same way to form a layer atop the frozen $KHCO_3$ solution. This process was repeated about ten times to increase the ice's thickness. Subsequent warming of the sample to ~ 200 K removed the H_2O and initiated a reaction between HBr and $KHCO_3$ to form H_2CO_3, changes that were followed with IR spectroscopy. The sample then was heated to 240 - 255 K, and IR spectra recorded over time, with a focus on the 1300 and 1500 cm^{-1} features of H_2CO_3. Band areas were measured and combined with intrinsic band strengths, so called *A* values, to determine the vapor pressures and enthalpy of sublimation (ΔH_{sub}) of H_2CO_3 (Khanna et al., 1990). These measurements were made with a Mattson Polaris spectrometer operating in a conventional transmission mode.

3.2. Radiolytic destruction

The destruction of crystalline H_2CO_3 by 0.8 MeV protons was followed by measuring the decrease in IR band areas after various doses. As an example, Figs. 3a and 3b compare spectra in the 2900 – 1500 cm^{-1} (3.45 – 6.67 μm) region before and after irradiation to a dose of 2.0 eV $molecule^{-1}$. The H_2CO_3 bands are seen to decrease, indicating a loss of molecules, and at the same time H_2O and CO_2 are formed (H_2O is not shown). In addition, irradiation caused the H_2CO_3 bands to widen, indicating amorphization of the crystalline sample.

To accurately quantify carbonic acid's radiolytic destruction it was necessary to distinguish between spectral changes caused by (a) loss of H_2CO_3 molecules and (b) amorphization. This was done by warming the sample to 200 K after each irradiation step to fully recrystallize the partially-amorphous ice and to sublime away the H_2O and CO_2 formed by radiolysis. The ice then was recooled to 14 K, as shown in Fig. 3c, for comparison to the original spectrum of the unirradiated ice, Fig. 3a. The spectra of Figs. 3a and 3c are similar, but the latter has slightly smaller H_2CO_3 bands, caused by the destruction of crystalline H_2CO_3.

The normalized band areas for H_2CO_3 have been plotted in Fig. 4 as a function of radiation dose. Table 2 lists all bands that were averaged for this graph along with their integration limits. Also in Fig. 4 are linear regression lines through the data points. The corresponding half-life doses for H_2CO_3 irradiated at 14, 100, and 200 K are then 11, 11, and 7 eV $molec^{-1}$, respectively.

temperature. After this annealing cycle, some CO_2 often remained trapped in the H_2CO_3 (Fig. 3c). In order to relate only the amount of CO_2 formed to the amount of H_2CO_3 destroyed, at each radiation step we subtracted the band area of any remaining CO_2 in the annealed ice from the area of the CO_2 band recorded after the next irradiation. Table 3 gives the results of these $A(H_2CO_3)$ measurements at 14 and 100 K, corrected for amorphization. Because most of the CO_2 product immediately sublimed away upon formation at 200 K, no band strengths were determined at that temperature. Note that the measurements in Table 3 are based on $A(CO_2) = 7.6 \times 10^{-17}$ cm molec^{-1} (Gerakines et al., 1995), and that no decomposition of H_2CO_3 into CO appeared to occur. A few experiments with $H_2{}^{13}CO_3$ were conducted to verify that all of the CO_2 formation observed in our work was due to the proton irradiation, and not from leaks in the vacuum system. No such contamination was detected in any experiment.

3.4. Radiation yield of H_2CO_3

The radiation-chemical yield, denoted G, of a substance is the number of molecules produced by absorption of 100 eV. Previously-reported values for $G(H_2CO_3)$ from $H_2O + CO_2$ (1:1) ices at 14 K were 0.028, 0.030, and 0.02 for MeV protons and UV photons (Gerakines et al., 2000), and for 10 keV electrons (Hand et al., 2007), respectively. These values were based on the growth of H_2CO_3 IR bands as a function of radiation dose, and represent the formation of H_2CO_3 within an amorphous ice mixture dominated by H_2O and CO_2. We repeated this type of experiment by irradiating $H_2O + CO_2$ (1:1) at 14 K and 50 K in small steps, the 1500 cm^{-1} band's area being measured after each irradiation. The column density of H_2CO_3 was calculated from equation (1)

and this may account for the 8 – 18 cm^{-1} shift of some bands with respect to their positions in the radiation-formed H_2CO_3.

Figure 6 shows the decrease in the normalized average areas for the 1300 and 1500 cm^{-1} bands of H_2CO_3 as a function of time at five different temperatures. Each decrease is related to a change in column density, the number of molecules per cm^2 leaving the ice surface as a function of time. To determine column densities we used *A* values measured at 100 K. The slopes of similar non-normalized plots gave the sublimation fluxes (molec m^{-2} sec^{-1}) at each temperature. Equation (4) then was used to calculate the vapor pressure, p.

$$\text{Sublimation Flux} = p / (2\pi mkT)^{1/2} \qquad (4)$$

In (4), m is the mass of an H_2CO_3 molecule, k is the Boltzmann constant, and T is the absolute temperature, giving a vapor pressure in Newtons m^{-2}, which was converted to units of bar. A plot of the calculated vapor pressure from 238 to 256 K is shown in Fig. 7a. Figure 7b shows the same data graphed as ln(p) versus 1/T, from which the slope gives the heat of sublimation as $\Delta H_{sub} = 65.2$ kJ mol^{-1}.

3.6. Chemical destruction

In addition to measurements of both the sublimation and the radiolytic destruction of solid H_2CO_3, we also have observed H_2CO_3 loss by chemical reaction. Previously, we found that ammonia (NH_3) blocks H_2CO_3 formation in irradiated solid-phase $H_2O + CO_2 + NH_3$ mixtures (Gerakines et al., 2000). In separate experiments, we have irradiated layered samples consisting of a mixture of solid $H_2O + CO_2$ over a layer of NH_3, both ices being formed at ~ 10 K. Subsequent irradiation produced H_2CO_3 in the upper layer,

5 shows the results of such a calculation, giving a half-life for carbonic acid at 100 K on both Europa and Callisto.

The spectra we have recorded, such as in Fig. 1, illustrate the differences between carbonic acid in an amorphous matrix and pure crystalline H_2CO_3. On warming from 14 to 240 K (Figs. 1b and 1c), some peaks shift, some bands narrow, and some splittings are observed. As an example, the broad, weak band near 2555 cm^{-1} (3.914 μm) sharpens considerably and moves to 2612 cm^{-1} (3.828 μm) on warming to 240 K. Figure 2 shows that this same feature then displays small, reversible shifts in position as the temperature of the carbonic acid is changed. The importance of documenting such spectral variations is demonstrated by Fig. 9, which overlays this same OH stretching feature of carbonic acid on reflectance spectra of Callisto and Europa. The spectrum of pure crystalline H_2CO_3 is shown as is one in which carbonic acid is trapped in an amorphous ice mixture. It is seen that the band shape and position for the amorphous ice provides the better fit. Any similar feature on Europa is within the noise of the data as demonstrated in Fig. 9. See Johnson et al. (2004) for a suggestion of H_2CO_3 as a possible candidate for Callisto. Additional details on the shifts and intensity changes of H_2CO_3 features can be found in Winkel et al. (2007).

Our analysis of data from irradiated H_2CO_3 considers both radiation-induced chemistry and radiation-induced amorphization. Separating these effects is important because measurements of both H_2CO_3 loss and CO_2 growth are needed for an accurate determination of intrinsic IR band strengths of carbonic acid. Along these lines, the band strengths we report in Table 3 are significantly different (> 50%) from some of the older, uncorrected values.

(25.2 kJ mol^{-1}), which will assist H_2CO_3 in remaining on planetary surfaces after the sublimation of the other two molecules. For comparison to other carboxylic acids, ΔH_{sub} is 62.5 kJ mol^{-1} for formic acid (HCOOH) and 67.9 kJ mol^{-1} for acetic acid (CH_3COOH). See Calis-Van Ginkel et al. (1978).

Having discussed our results, it is appropriate to point out some limitations and possible future work. Two sources of error in Table 1 are the unknown density and radiation stopping power of a 1:1 $H_2O + CO_2$ ice. Our approach was simply to assume these quantities to be an average of the values of the individual components. A direct measurement, particularly of the density, is desirable.

The H_2CO_3 formation we report is for this molecule generated in an amorphous mixture of $H_2O + CO_2$ (1:1). However, to quantify carbonic acid production we were forced to use our *A* values for *crystalline* H_2CO_3. The reason for this is that neither of the synthetic techniques we used to prepare H_2CO_3 resulted in the pure amorphous material. To our knowledge, pure amorphous H_2CO_3 has not yet been made and so no spectra or band strengths are available. A related difficulty concerned the purity of the carbonic acid in our vapor pressure measurements. The acid-base reaction used to make H_2CO_3 gave KBr as a by-product. This is not expected to alter the vapor pressures of Fig. 7, but a check is desirable, such as with H_2CO_3 made by a different method.

We also note that our vapor-pressure work was done with an IR spectrometer operating in a conventional transmission mode, while measurements of radiolytic destruction utilized reflection spectroscopy. The spectra in the two cases were essentially identical, as seen in Fig. 5.

References

Brown, R. H., Clark, R. N., Buratti, B. J., Cruikshank, D. P., Barnes, J. W., Mastrapa, R. M. E., Bauer, J., Newman, S., Momary, T., Baines, K. H., and 15 coauthors, 2006. Composition and physical properties of Enceladus' surface. Science 311, 1425-1428.

Brucato J. R., Palumbo M. E., Strazzulla, G., 1997. H_2CO_3 by ion implantation in water/carbon dioxide ice mixtures. Icarus 125, 135-144.

Calis-Van Ginkel, C. H. D., Calis, G. H. M., Timmermans, C. W. M., DeKruif, C. G., Oonk, H. A. J., 1978. Enthalpies of sublimation and dimerization in vapor-phase of formic, acetic, propanoic and butanoic acids. J. Chem. Thermodyn. 1978, 10, 1083-1088.

Clark, R. N., Curchin, J. M., Jaumann, R., Cruikshank, D. P., Brown, R. H., Hoefen, T. M., Stephan, K., Moore, J. M., Buratti, B. J., Baines, K. H., Nicholson, P. D., Nelson, R. M., 2008. Compositional mapping of Saturn's satellite Dione with Cassini VIMS and implications of dark material in the Saturn system. Icarus 193, 372-386.

Cooper, J. F., Johnson, R. E., Mauk, B. H., Garrett, H. B., and Gehrels, N., 2001. Energetic ion and electron irradiation of the ice Galilean satellites. Icarus 149, 133-159.

DelloRusso, N., Khanna, R. K., Moore, M. H., 1993. Identification and yield of H_2CO_3 and formaldehyde in irradiated ices. J. Geophys. Res. E 98, 5505-5510.

Grundy, W. M., Young, L. A., Spencer, J. R., Johnson, R. E., Young, E. F., Buie, M. W., 2006. Distributions of H_2O and CO_2 ices on Ariel, Umbriel, Titania, and Oberon from IRTF/SpeX observations. Icarus 184, 543-555.

Hage, W., Hallbrucker, A., Mayer, E., 1993. Carbonic acid: synthesis by protonation of bicarbonate and FTIR spectroscopic characterization via a new cryogenic technique. J. Am. Chem. Soc. 115, 8427-8431.

Hand, K. P., Carlson, R. W, Chyba, C. F., 2007. Energy, chemical disequilibrium, and geological constraints on Europa. Astrobiology 7, 1006-1022.

Hansen, G. B., McCord, T. B., 2008. Widespread CO_2 and other non-ice compounds on the anti-Jovian and trailing sides of Europa from Galileo/NIMS observations. Geophys. Res. Lett. 35, L01202.

Hibbitts, C. A., McCord, T. B., Hansen, G. B., 2000. Distributions of CO_2 and SO_2 on the surface of Callisto. J. Geophys. Res. - Planets. 105, 22541-22558.

Hibbitts, C. A., Pappalardo, R. T., Hansen, G. B., McCord, T. B., 2003. Carbon dioxide on Ganymede. J. Geophys. Res. - Planets. 108, ID 5036.

Hudson, R. L., Moore, M. H., 2004. Reactions of nitriles in ices relevant to Titan, comets, and the interstellar medium: Formation of cyanate ion, ketenimines, and isonitriles. Icarus 172, 466-478.

Johnson, R. E., Carlson, R. W., Cooper, J. F., Paranicas, C., Moore, M. H., Wong, M. C., 2004. Radiation effects on the surfaces of the Galilean satellites. In: Bagenal, F., Dowling, T. E., McKinnon, W. B. (Eds.), Jupiter. The planet, satellites, and magnetosphere, vol. 1, Cambridge University Press, Cambridge, UK, 485-512.

Winkel, K., Hage, W., Loerting, T., Price, S., Mayer, E., 2007. Carbonic acid: From polyamorphism to polymorphism. J. Am. Chem. Soc. 129, 13863–13871.

Wu, C. Y. R., Judge, D. L., Cheng, B., Yih, T., Lee, C. S., Ip, W. H., 2003. Extreme ultraviolet photolysis of CO_2 – H_2O mixed ices at 10 K. JGR-Planets. 108, 13-1 – 13-8.

Zheng, W., Kaiser, R. I., 2007. On the formation of carbonic acid (H_2CO_3) in solar system ices. Chem. Phys. Lett. 450, 55-60.

Ziegler, J. P., Biersack, J. P., Littmark, U., 1985. The stopping and range of ions in solids. Pergamon, New York. See also http://www.srim.org.

Figure 5. A comparison of the IR spectra of H_2CO_3 formed by the irradiation of an H_2O + CO_2 (1:1) ice and the acid-base reaction of warmed HBr + $KHCO_3$. The upper spectrum was taken with the reflection method described in the text, while the lower spectrum was recorded in a conventional transmission mode.

Figure 6. Normalized areas (averaged) of the 1300 and 1500 cm^{-1} bands of H_2CO_3 plotted as a function of time for five different temperatures. Each point is from the average area of the IR bands at 1300 and 1500 cm^{-1}.

Figure 7. The vapor pressures of H_2CO_3 at five temperatures are shown. The slope of the regression line in the lower graph gives the heat of sublimation, ΔH_{sub} = 65.2 kJ mol^{-1}.

Figure 8. The IR spectrum of the H_2CO_3 + NH_3 solid-phase reaction product compared to room-temperature ammonium carbonate, $(NH_4)_2CO_3$.

Figure 9: The IR reflection spectra of Europa and Callisto compared to spectra of crystalline H_2CO_3 at 140 K and H_2CO_3 mixed with H_2O and CO_2 at 150 K. The H_2CO_3 absorbance spectra were inverted and arbitrarily scaled for this comparison. Callisto's observed 3.880 μm (2577 cm^{-1}) feature is more similar to that of H_2CO_3 held in the amorphous ice.

Figure 2

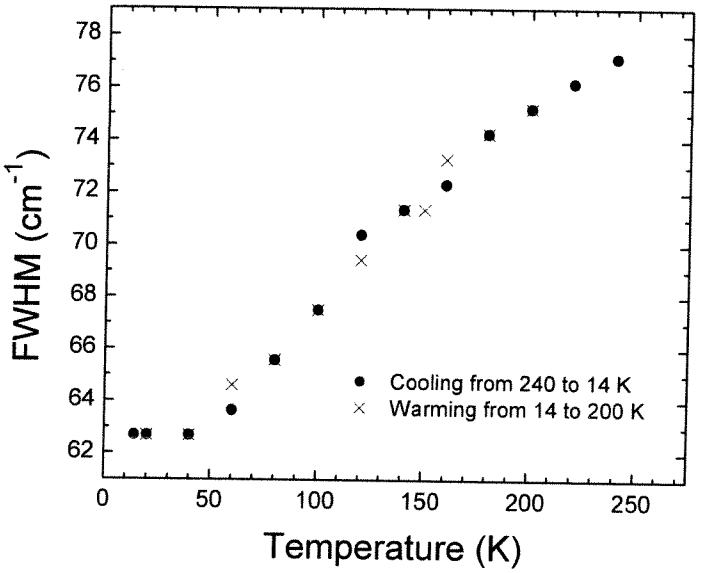
FWHM (cm^{-1})
78
76
74
72
70
68
66
64
62
0
50
100
150
200
250
Temperature (K)
Cooling from 240 to 14 K
Warming from 14 to 200 K

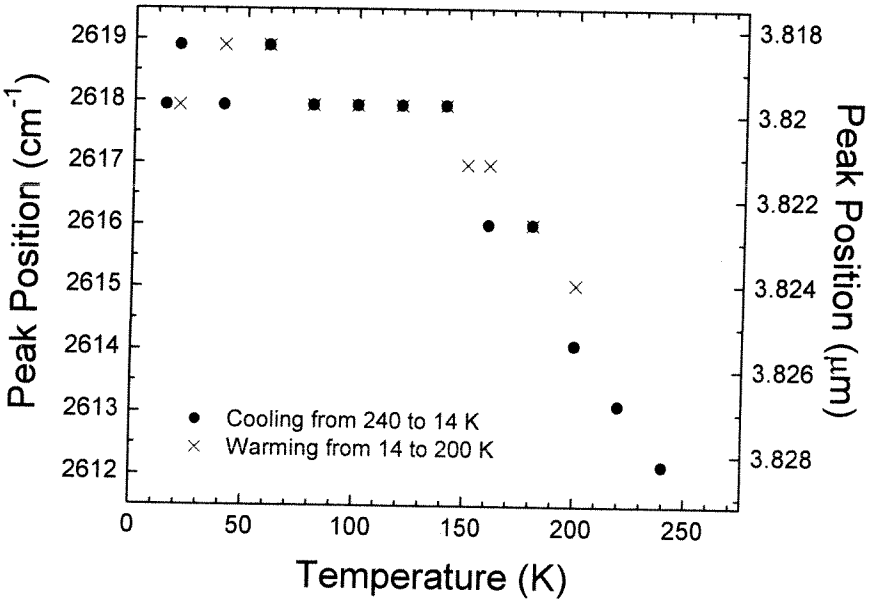
Peak Position (cm^{-1})
2619
2618
2617
2616
2615
2614
2613
2612
Peak Position (μm)
3.818
3.82
3.822
3.824
3.826
3.828
0
50
100
150
200
250
Temperature (K)
Cooling from 240 to 14 K
Warming from 14 to 200 K

Figure 4

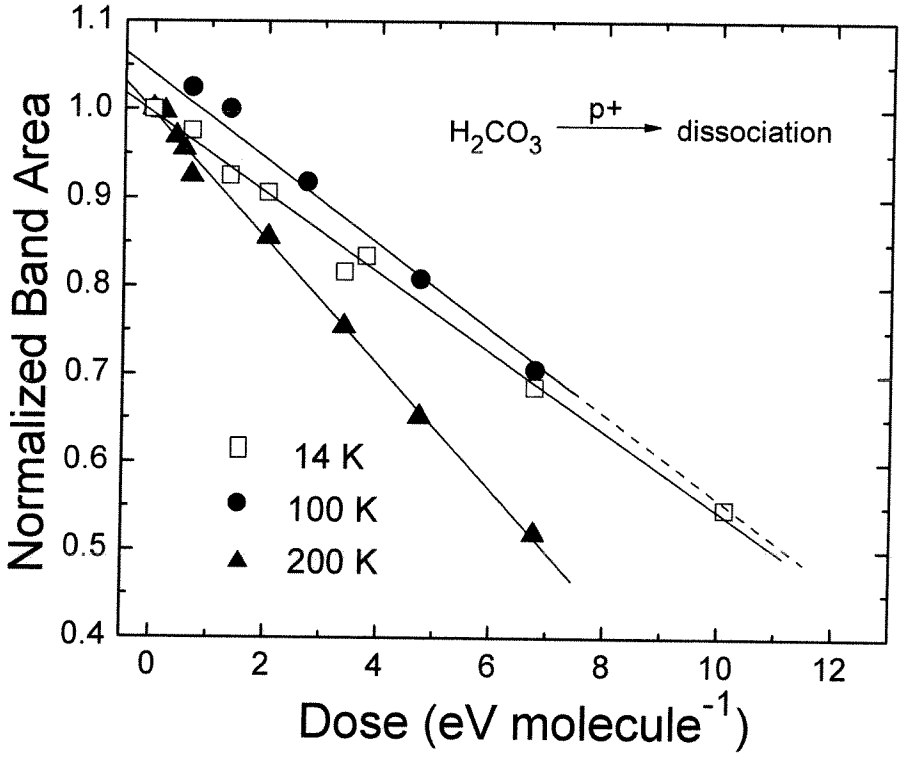
Normalized Band Area
Dose (eV molecule^{-1})
H_2CO_3 p+ dissociation
14 K
100 K
200 K
1.1
1.0
0.9
0.8
0.7
0.6
0.5
0.4
0
2
4
6
8
10
12

Figure 6

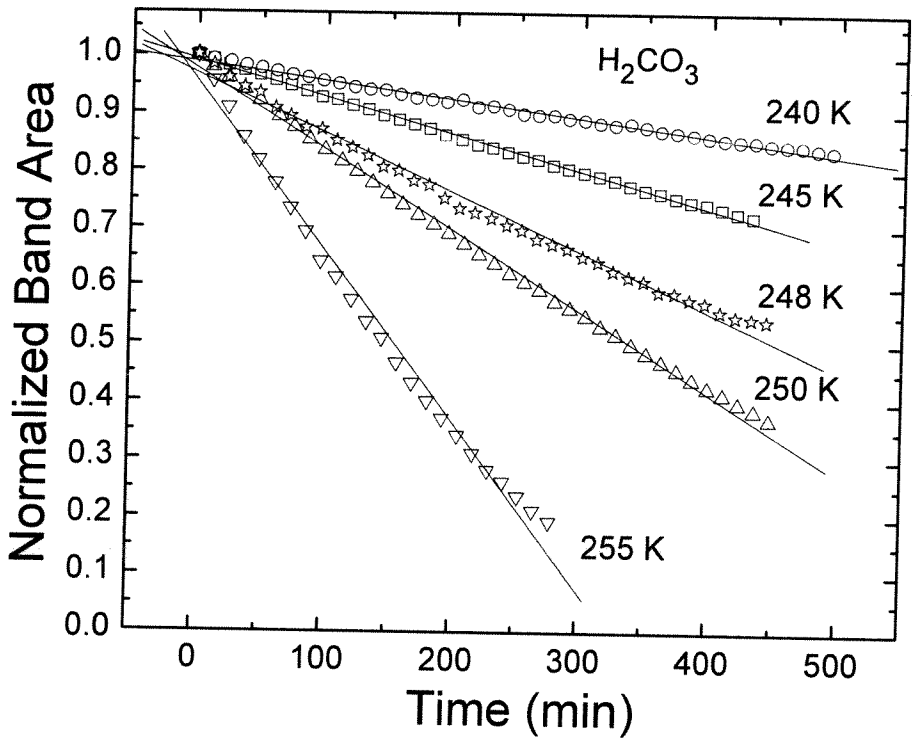
Normalized Band Area
1.0
0.9
0.8
0.7
0.6
0.5
0.4
0.3
0.2
0.1
0.0
0
100
200
300
400
500
Time (min)
H_2CO_3
240 K
245 K
248 K
250 K
255 K

Figure 8

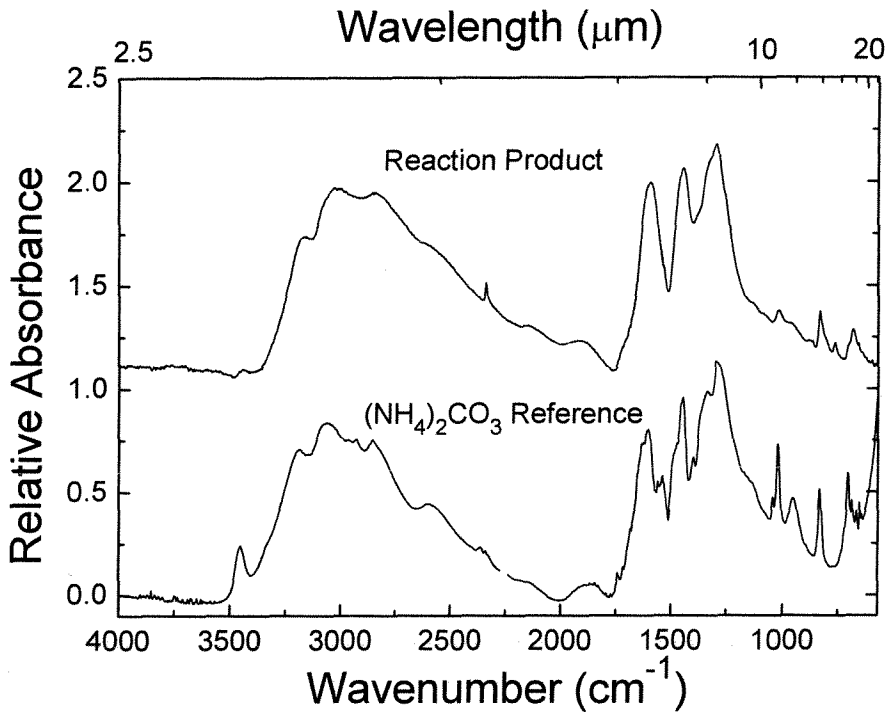
Wavelength (μm)
2.5
10
20
Reaction Product
(NH4)2CO3 Reference
Relative Absorbance
2.5
2.0
1.5
1.0
0.5
0.0
4000
3500
3000
2500
2000
1500
1000
Wavenumber (cm-1)

Table 1

Physical properties of ices

Ice	Molecular Mass ($g\ mol^{-1}$)	Density ($g\ cm^{-3}$)	Proton Stopping Power ($MeV\ cm^2\ g^{-1}$)[c]
H_2O	18	1	273
CO_2	44	1.7	240
$H_2O + CO_2$ (1:1)	31	1.35[a]	256.5[a]
H_2CO_3	62	1[b]	254

[a]Average value for a $H_2O + CO_2$ (1:1) mixture.

[b]Assumed value.

[c]Calculated for 0.8 MeV protons, according to method of Zeigler et al. (1985).

Table 3

IR band positions and strengths (A) for H_2CO_3 at 14 and 100 K

Band Position		$A(10^{-17}$ cm molec$^{-1})$			
Wavenumber (cm^{-1})	Wavelength (μm)	14 K	100 K	18 K[a]	185 K[b]
2749 + 2833	3.634 + 3.530	5.3	3.3	9.8	--
2618	3.820	7.5	7.2	16.0	--
1695	5.900	10.8	14.8	11	35
1503	6.653	5.2	9.1	6.5	11
1303	7.675	8.5	12.3	10	12.6
1038	9.634	0.15	0.17	0.14	--
875	11.43	4.5	2.8	5.6	--

[a]From 18 K photodissociation of H_2CO_3 (Gerakines et al., 2000).

[b]From 185 K implantation of H^+ into CO_2 ice to form H_2CO_3 (Garozzo et al., 2008).

Table 5

Half-lives for crystalline H_2CO_3, based on the 100 K destruction rate in the laboratory, corrected for amorphization

Environment	Depth (μm)	Volume Dose Rate (eV molec^{-1} s^{-1})	Half-Life
Laboratory	1.0	1.3×10^{-3}	2.4 h
Europa[a]	100	1.0×10^{-8}	35 y
Callisto[a]	100	2.5×10^{-11}	1.4×10^{4} y

[a]Volume dose rates for Europa and Callisto from Cooper et al. (2001).